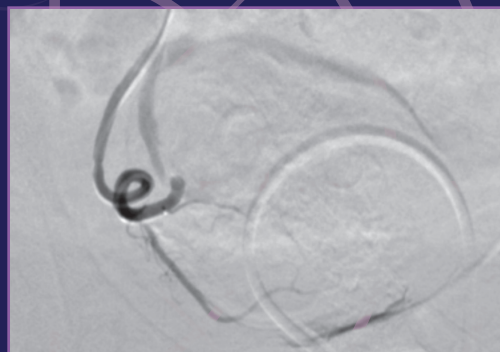
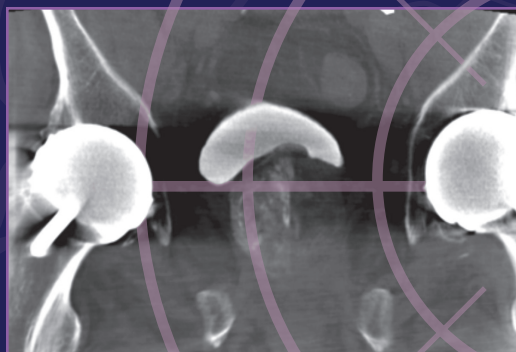
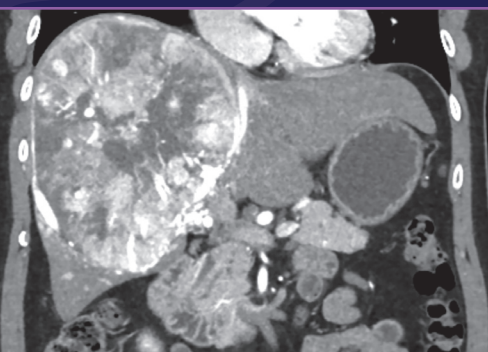


Endovascular TODAY

January 2020



CASE STUDIES IN EMBOLIZATION

Using the SeQure[®] Microcatheter



Table of **CONTENTS**

**3 Chemoembolization Via Intrahepatic
Collateral Arteries**

By Daniel Y. Sze, MD, PhD

6 Prostate Artery Embolization

By Ari J. Isaacson, MD

8 Uterine Artery Embolization

By Aaron Rohr, MD, MS

All authors were compensated by Guerbet for their contributions. Dr. Sze is a consultant to Guerbet.

Chemoembolization Via Intrahepatic Collateral Arteries

BY DANIEL Y. SZE, MD, PhD

CASE SUMMARY

A 53-year-old man with chronic hepatitis B presented with elevated transaminases while taking herbal supplements, but was otherwise asymptomatic, Child-Pugh A5, and ECOG performance status 0. Workup included nonreactive hepatitis B surface antigen, negative hepatitis C antibody, negative colonoscopy except for small hemorrhoids, negative antinuclear antibody, negative alpha-1 antitrypsin, and ceruloplasmin tests. He transferred his care to a second hospital and underwent hepatic ultrasonography, revealing a 16-cm mass, confirmed on multiphase CT scan to be a hepatocellular carcinoma (Figure 1). He then transferred his care to a tertiary care hospital, where he underwent a trisegmentectomy.

One year after “curative” resection, follow-up imaging revealed a hypervascular lesion in segment 3 measuring 2.1 cm, indicative of recurrence (Figure 2). A second possible lesion in the fissure of the ligamentum venosum was measured at 0.8 cm and was felt to be inaccessible for ablation (Figure 2). The patient’s liver function remained Child-Pugh A5, but his performance

status had deteriorated mildly to status 1 after surgery. He was referred for hepatic angiography and chemoembolization.

IMAGING FINDINGS

Initial hepatic angiography revealed postsurgical distortion of the arterial anatomy, with proximal occlusion of the segment 2 and segment 3 arteries with distal reconstitution from intrahepatic collateral vessels (Figure 3). Parenchymal phase imaging confirmed two hypervascular lesions (Figure 3).

Although the collateral vessels appeared too small in diameter and too tortuous to accommodate standard

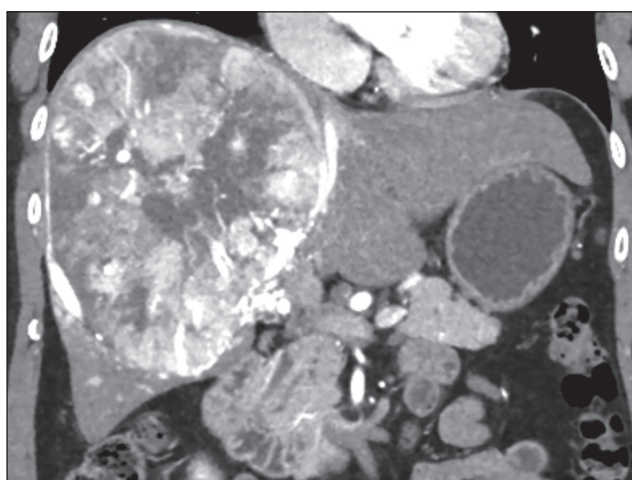


Figure 1. Coronal reformat of arterial-phase CT shows replacement of the right lobe with a large hepatocellular carcinoma, extending into segments 1 and 4.

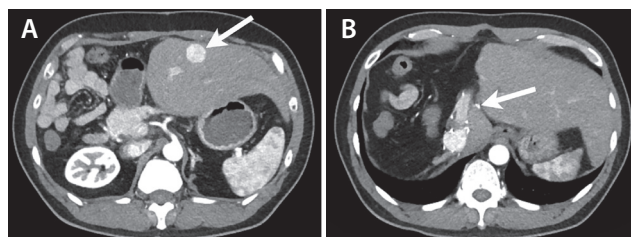


Figure 2. Arterial-phase CT image of the remnant liver 1 year after resection shows a new 2.1-cm lesion in segment 3 (arrow). Washout and pseudocapsule confirmed recurrent hepatocellular carcinoma (A). A second small nodule of hypervascularity is seen in the fissure of the ligamentum venosum adjacent to the left portal vein (arrow) but is too small to characterize further (B).

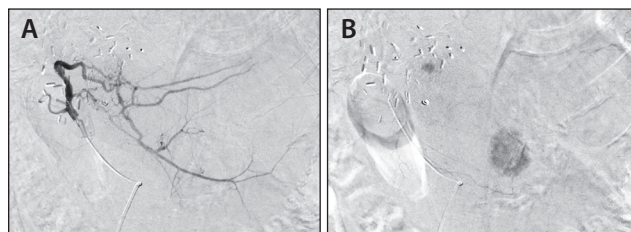


Figure 3. Left hepatic arteriogram revealed occlusion of the proximal segment 2 and segment 3 branches, with reconstitution of distal branches via intrahepatic collateral vessels at the cut surface (A). Parenchymal phase image from the same arteriogram confirmed two hypervascular lesions (B).

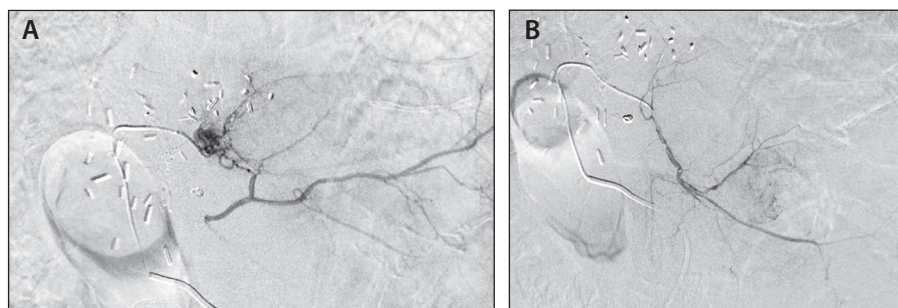


Figure 4. Selective arteriogram of the most cranial segment 2 collateral branch confirmed supply to the smaller lesion. A 2.8-Fr SeQuire® catheter was wedged into this submillimeter vessel, and harder injection showed additional collateralization reconstituting distal segment 2 vessels (A). Selective arteriogram of the largest but most tortuous collateral vessel reached the reconstituted segment 3 vessel, supplying the larger tumor (B).

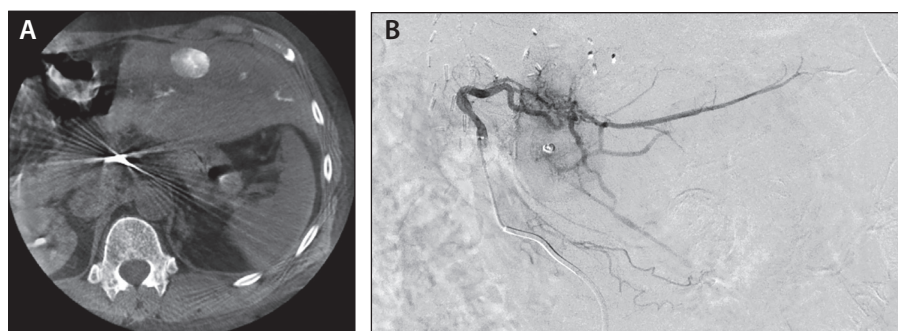


Figure 5. After administration of 100–300-µm doxorubicin-eluting microspheres at both sites, the final arteriogram showed resolution of tumor blushes and retained patency of the collateral network, segment 2 artery, and proximal segment 3 artery (A). Unenhanced cone-beam CT showed retention of iodinated contrast medium in the tumors, as well as in some peripheral arteries (B).

microcatheters, treatment was attempted using a Fathom 0.014-inch guidewire (Boston Scientific Corporation) and a 2.8-Fr SeQuire® microcatheter (Guerbet). (At the time, smaller-diameter SeQuire® microcatheters had not yet been released.)

The submillimeter branch supplying the falciform cleft was successfully selected, and the lesion was treated with doxorubicin-loaded LC beads 100–300 µm (BTG) until stasis of the tumor-feeding branch (Figure 4) was achieved. Likewise, the tortuous intrahepatic collateral vessel to segment 3 was selected and the segment 3 lesion was also treated with drug-eluting LC beads (Figure 4). Completion angiography confirmed disappearance of tumor blushes but maintenance of flow in nontarget vessels (Figure 5), and unenhanced cone-beam CT confirmed retention of contrast medium in the treated lesions (Figure 5).

Follow-up MRI at 3 months revealed complete response of the ligamentum venosum lesion and partial response of the segment 3 lesion. Residual disease was treated with percutaneous microwave ablation.

DISCUSSION

Microcatheter design must balance the demands of: (1) adequate lumen to accommodate viscous or particle-containing injected fluids; (2) flexibility to navigate tortuosities without causing vessel injury; and (3) longitudinal stiffness to allow pushability. Additional features may include shaped tips, torqueability, and characteristics that help reduce reflux.

CONCLUSION

Selectivity of catheterization and treatment has a substantial impact on outcomes of transarterial chemoembolization. Navigation of small, tortuous vessels is possible using the SeQuire® microcatheter, even using the large 2.8-Fr version. Although this case cannot demonstrate the reflux reduction features of the SeQuire® microcatheter, it demonstrates the flexibility and pushability that allowed selection of small, tortuous vessels. Future studies using

radiopaque microspheres may be performed to test the controlled reflux feature. ■

Recommended Reading

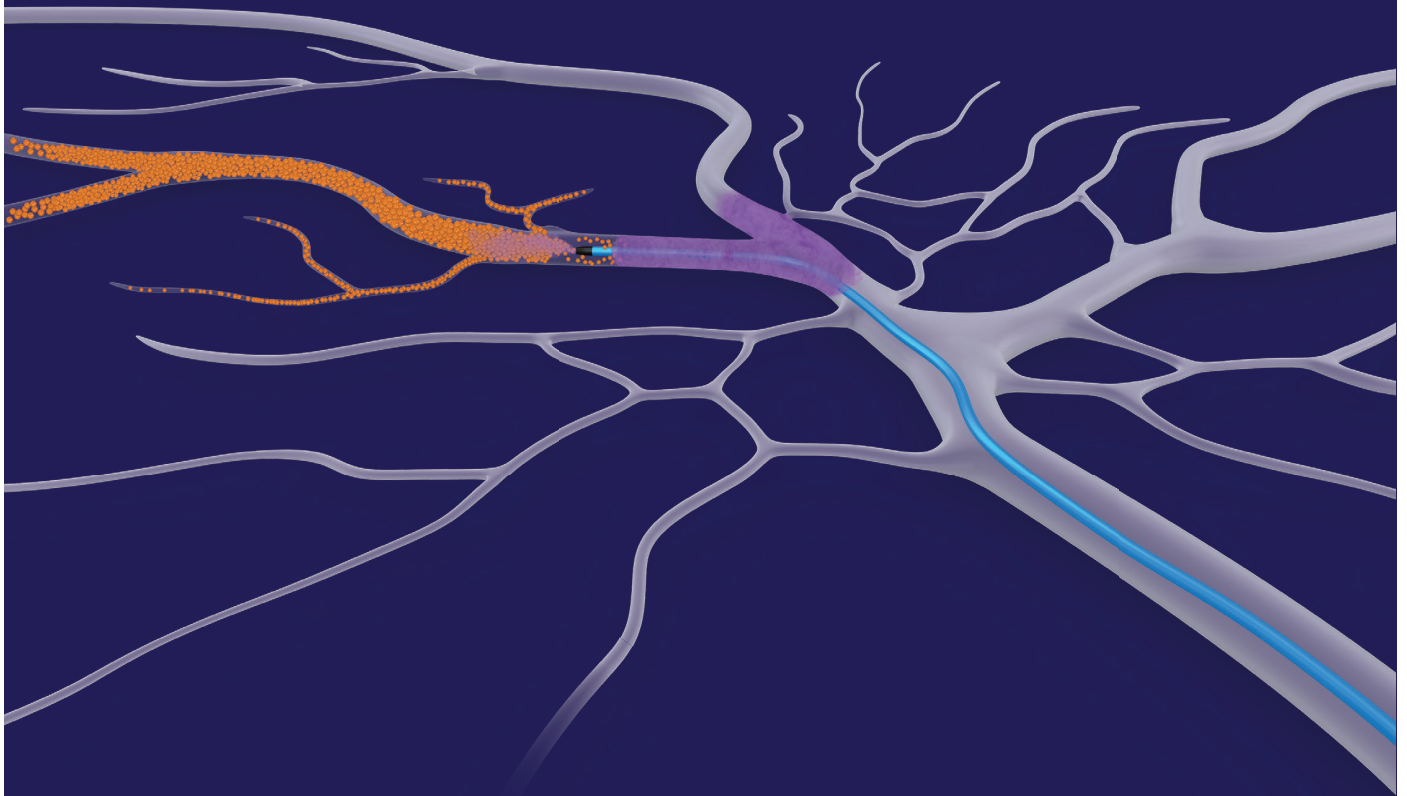
1. Miyayama S, Mitsui T, Zen Y, et al. Histopathological findings after ultraslective transcatheter arterial chemoembolization for hepatocellular carcinoma. *Hepatol Res*. 2009;39:374–381.
2. Mokin M, Waqas M, Setlur Nagesh SV, et al. Assessment of distal access catheter performance during neuroendovascular procedures: measuring force in three-dimensional patient specific phantoms. *J Neurointerv Surg*. 2019;11:619–622.
3. Ogata N, Goto K, Uda K. An evaluation of the physical properties of current microcatheters and guidewires. The development of the “catheter-glide approach” in response to weaknesses of current materials. *Interv Neuroradiol*. 1997;3:65–80.
4. Zoarski GH, Mathis JM, Hebel JR. Performance characteristics of microcatheter systems in a standardized tortuous pathway. *AJNR Am J Neuroradiol*. 1998;19:1571–1576.

Daniel Y. Sze, MD, PhD

Professor of Vascular and Interventional Radiology
Stanford University
Stanford, California

SEQURE®
Reflux Control Microcatheter

**Designed to reduce
microspheres reflux**



Guerbet | 

Prostate Artery Embolization*

BY ARI J. ISAACSON, MD

CASE SUMMARY

A 61-year-old man presented with a 15-year history of urinary symptoms secondary to benign prostatic hyperplasia (BPH). He had a known prostate size of 70 g (normal, 20–30 g), and his chief complaint was hesitancy and intermittency of urination. Initially, he was treated with medications for his symptoms (tamsulosin and finasteride), but treatment was discontinued due to sexual side effects. After failure to improve using herbal/holistic supplements to relieve his symptoms, he found his symptoms were having a significant negative effect on his quality of life (QOL). However, he was wary of pursuing a surgical solution such as transurethral resection of the prostate, because of the potential side effects associated with the procedure. Instead, he decided to undergo prostate artery embolization (PAE).

DIAGNOSIS

Urinary symptoms secondary to BPH

IMAGING FINDINGS/RESULTS

The patient underwent PAE from a femoral artery approach (as he was too tall for a radial artery approach). To begin, a 5-Fr catheter was placed into his left internal iliac artery, and angiography demonstrated that his prostatic artery arose from the internal pudendal artery. (Note: the patient also had a history of bilateral hip arthroplasty, as is evident on the images.) Prior to embolization, an arterial anastomosis to the rectum was coil-embolized with a 3/2-mm Tornado® Embolization Coil (Cook Medical). Additionally, an arterial anastomosis to the internal pudendal artery was embolized with a similar coil.

At that point, a 2.4-Fr SeQuire® microcatheter (Guerbet) was inserted into the left prostatic artery, and the left hemi-prostate was embolized with 250 µm Embozene™ Microspheres (Boston Scientific Corporation) until flow was sluggish, at which point, embolization was completed with a gelfoam slurry. When using the SeQuire® catheter, the embolic solution can become more concentrated as the fluid component exits the holes within the distal catheter; therefore, we recommend the initial solution be adequately diluted to prevent aggregation and



Figure 1. Digital subtraction angiography with the SeQuire® microcatheter positioned distally in the right prostatic artery (arrow), demonstrating the characteristic blush of the right hemi-prostate.

occlusion of the catheter. A Waltman loop maneuver was then used to select the right internal iliac artery with the 5-Fr catheter. Angiography was again performed, demonstrating the right prostatic artery arising from a vesicoprostatic trunk. The SeQuire® microcatheter was then reinserted, and more selective angiography demonstrated the right hemi-prostatic blush (Figure 1). Embolization was performed with 250-µm particles. When flow was once again sluggish, embolization was completed with the gelfoam slurry.

After the catheters were removed, noncontrast, cone-beam computed tomography (CT) demonstrated contrast retention throughout the prostate, suggesting complete embolization (Figure 2).

DISCUSSION

The SeQuire® catheter was designed to reduce premature embolic reflux during embolization procedures. In this case, after initial embolization,

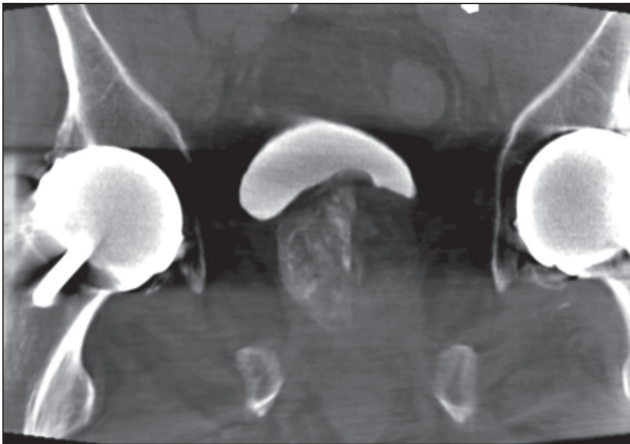


Figure 2. Coronal image from a noncontrast cone-beam CT after embolization, demonstrating retained contrast throughout the prostate. The increased density seen in the right hemi-prostate is due to the fact that it was embolized after the left and, therefore, less of the contrast had been resorbed.

contrast was observed exiting through the side hole at the distal segment of the catheter, creating the protective pressure gradient and preventing reflux (Figure 3). This potentially results in more particles being injected into the prostate compared to a standard end-hole catheter. The final cone-beam CT images suggest that this catheter is capable of thorough embolization of the prostate.

Importantly, the patient was evaluated before and after the procedure for symptom severity using the International Prostate Symptom Score (IPSS) questionnaire, an 8-question tool used to screen for, diagnose, and track symptoms of BPH. The IPSS has seven questions related to symptoms and one related to QOL. In this case, the patient's baseline IPSS was 25 (on a scale of 1 to 35; 25 is severely symptomatic) and his QOL was 4 (on a scale of 0 to 6; 4 is mostly dissatisfied). Three months postprocedure, his IPSS score was 10 (low-to-moderately severe) and his QOL score was 1 (pleased), indicating that PAE performed with a SeQuire® catheter successfully alleviated this patient's symptoms.

CONCLUSION

PAE performed with a SeQuire® catheter is an emerging interventional technique that can be used successfully to manage patients with urinary tract symptoms secondary to BPH. ■

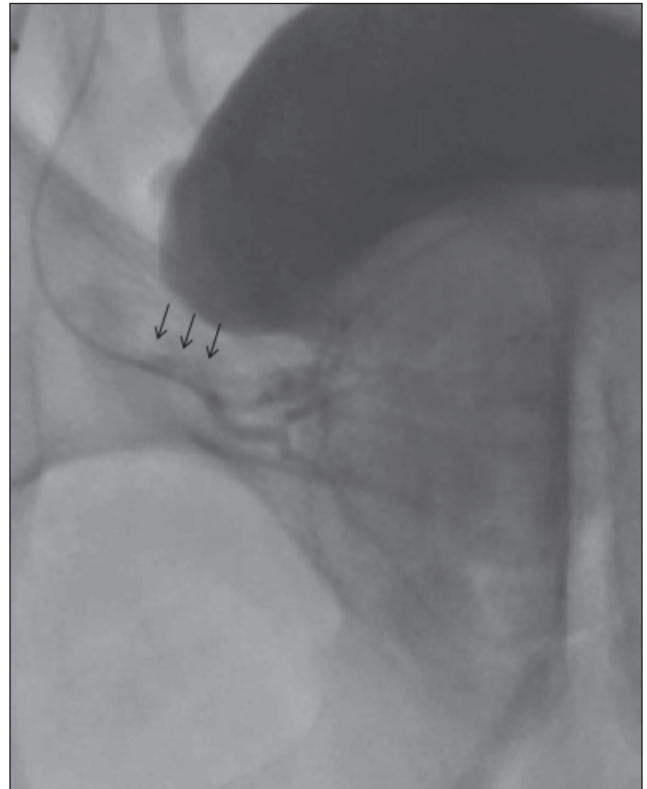


Figure 3. Fluoroscopic image demonstrating embolization of the right hemi-prostate. Contrast can be seen exiting the holes in the distal segment of the microcatheter forming the anti-reflux pressure gradient (arrows).

Recommended Reading

1. Gao YA, Huang Y, Zhang R, et al. Benign prostatic hyperplasia: prostatic arterial embolization versus transurethral resection of the prostate—a prospective, randomized, and controlled clinical trial. *Radiology*. 2014;270:920-928.
2. Pisco JM, Bilhim T, Pinheiro LC, et al. Medium- and long-term outcome of prostate artery embolization for patients with benign prostatic hyperplasia: results in 630 Patients. *J Vasc Interv Radiol*. 2016;27:1115-1122.
3. Ray AF, Powell J, Speakman MJ, et al. Efficacy and safety of prostate artery embolization for benign prostatic hyperplasia: an observational study and propensity-matched comparison with transurethral resection of the prostate (the UK-ROPE study). *BJU Int*. 2018;122:270-282.
4. Uflacker A, Haskal ZJ, Bilhim T, et al. Meta-analysis of prostatic artery embolization for benign prostatic hyperplasia. *J Vasc Interv Radiol*. 2016;27:1686-1697.

*The SeQuire® microcatheter is not recommended for use with gelfoam.

Ari J. Isaacson, MD

Associate Professor, Vascular-Interventional Radiology
Director of Clinical Research, Department of Radiology
UNC School of Medicine
Chapel Hill, North Carolina

Uterine Artery Embolization

BY AARON ROHR, MD, MS

CASE SUMMARY

A 49-year-old perimenopausal female presented with a history of abnormal uterine bleeding, pelvic pain, prolonged menstruation, uterine fibroids, and metabolic syndrome. Pelvic ultrasound demonstrated increased size of numerous fibroids, including subserosal and intramural subtypes. The largest intramural fibroid measured 3.0 X 3.0 cm. The remaining sonographic examination was unremarkable, aside from a stable 1.7-cm right ovarian cyst. Endometrial biopsy was negative for malignancy; the patient had previously trialed intrauterine device hormonal therapy without symptom relief. She was then presented with treatment options such as uterine artery embolization (UAE), hysterectomy, and hormone therapy.¹ The patient elected to be treated with UAE and was referred to interventional radiology and surgery.²

DIAGNOSIS

Symptomatic uterine fibroids

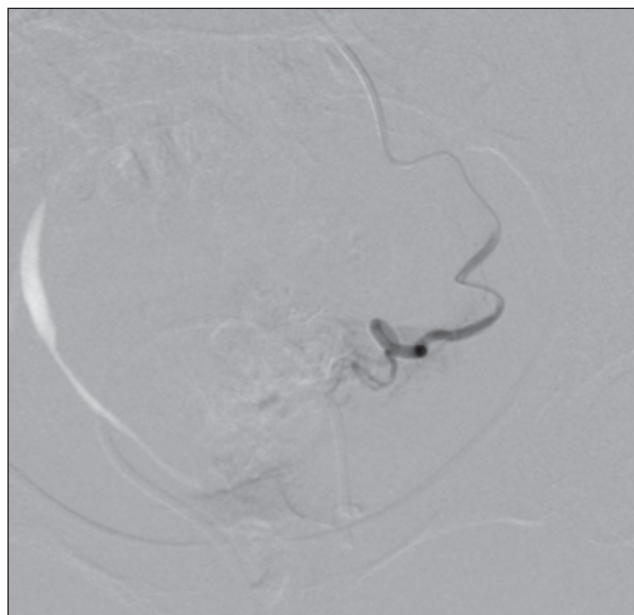


Figure 1. Angiography of the left uterine artery post bland embolization with complete stasis.

IMAGING FINDINGS

The patient underwent UAE utilizing the left radial artery approach.³ A 4/5-Fr slender sheath was placed into her left radial artery, followed by delivery of a vasodilator cocktail. The bilateral iliac arteries were cannulated with a 5-Fr Soft-Vu JB-1 catheter (AngioDynamics). Angiography demonstrated tortuous and engorged bilateral uterine arteries supplying the leiomyomatous uterus.

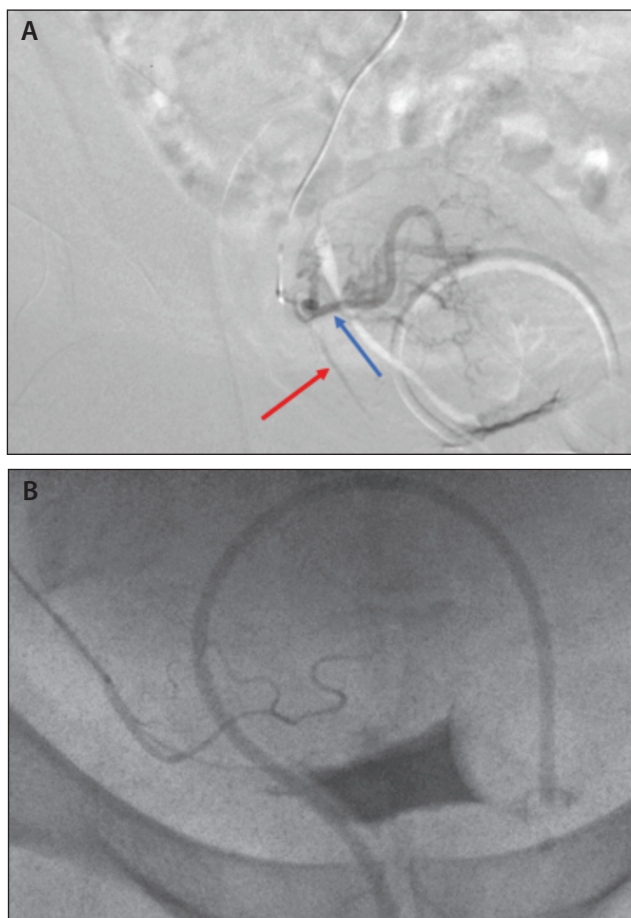


Figure 2. Initial angiogram of the right uterine artery demonstrating engorged and tortuous uterine artery (blue arrow), with inferior accessory cystic artery (red arrow) (A). Superselective arteriogram of accessory cystic artery off of the uterine artery (B).

After careful image-guided planning, the left uterine artery was selected via a 130-cm, 2.8-Fr SeQure® microcatheter (Guerbet). Initial arteriogram re-demonstrated tortuous and dilated uterine artery without evidence of collateral supply or accessory cystic artery. Bland embolization via 300–500- μ m Embospheres (Merit Medical) was administered via the left uterine artery. Postembolization angiography demonstrated complete stasis without evidence of contrast reflux (Figure 1).

The right uterine artery was then selected using the SeQure® microcatheter in a similar fashion. However, this angiogram demonstrated an additional single-vessel supply to the inferior margin of the bladder, most consistent with an accessory cystic artery (Figure 2). The SeQure® microcatheter was easily negotiated beyond the accessory cystic artery takeoff, through the tortuous right uterine artery. The right uterine artery was then embolized in a similar fashion with exclusion of the accessory vesicular artery, presumably via the unique flow-directed methodology of the SeQure® microcatheter. Complete stasis of the right uterine artery was noted postembolization, with complete preservation of the accessory cystic artery (Figure 3).

DISCUSSION

The SeQure® microcatheter was designed to assist with, and limit reflux during, flow-directed embolization procedures. In this case, the microcatheter was employed to deliver embolic agents to the bilateral uterine arteries in the setting of symptomatic fibroids.² Specifically, the microcatheter was able to isolate the right uterine artery and completely exclude the accessory cystic artery without requiring additional interventions, such as balloon occlusion, etc. This case demonstrates additional use of a microcatheter for excluding unwanted, nontargeted embolization in the appropriate clinical setting.

The SeQure® microcatheter provided excellent tracking ability through the uterine arteries in a

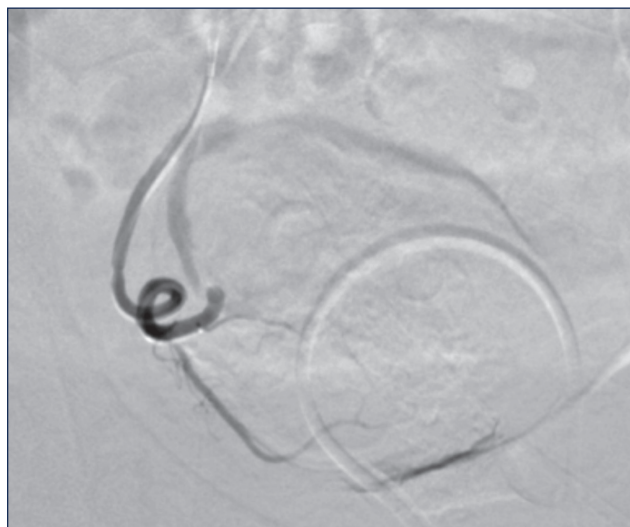


Figure 3. Digital subtraction angiogram of the right uterine artery demonstrating stasis with complete preservation of the accessory cystic artery.

well-controlled fashion without causing spasm of the associated artery.

CONCLUSION

UAE can be performed with a SeQure® microcatheter to successfully manage patients with symptomatic fibroids. ■

1. Mortensen C, Chung J, Liu D, et al. Prospective study on total fluoroscopic time in patients undergoing uterine artery embolization: comparing transradial and transfemoral approaches. *Cardiovasc Interv Radiol*. 2018;42:441–447.
2. Gupta JK, Sinha A, Lumsden MA, Hickey M. Uterine artery embolization for symptomatic uterine fibroids. *Cochrane Database Syst Rev*. 2012;CD005073.
3. Hirst A, Dutton S, Wu O, et al. A multi-centre retrospective cohort study comparing the efficacy, safety and cost-effectiveness of hysterectomy and uterine artery embolisation for the treatment of symptomatic uterine fibroids. The HOPEFUL study. *Health Technol Assess*. 2008;12:1–248, iii.

Aaron Rohr, MD, MS

Associate Professor, Vascular-Interventional Radiology
University of Kansas
Kansas City, Kansas

Optimized Trackability



Optimizing pushability, flexibility, and torqueability for improved trackability

Endovascular TODAY

For more information, please contact Customer Service at 877-729-6679 or customer.service-us@guerbet.com

Guerbet | 

GU11191276